Analytical Methods

Accepted Manuscript

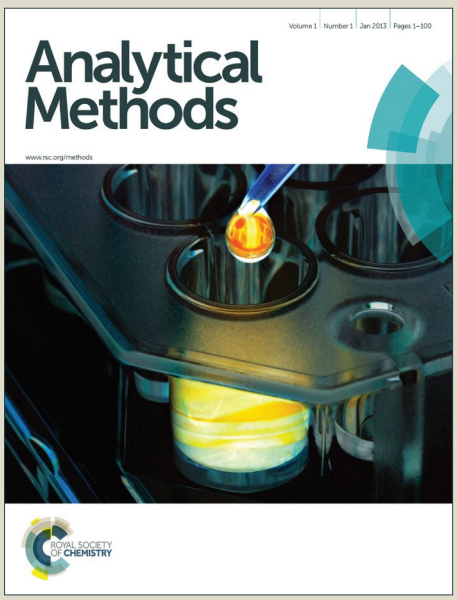

This is an *Accepted Manuscript*, which has been through the Royal Society of Chemistry peer review process and has been accepted for publication.

Accepted Manuscripts are published online shortly after acceptance, before technical editing, formatting and proof reading. Using this free service, authors can make their results available to the community, in citable form, before we publish the edited article. We will replace this *Accepted Manuscript* with the edited and formatted *Advance Article* as soon as it is available.

You can find more information about *Accepted Manuscripts* in the Information for Authors.

Please note that technical editing may introduce minor changes to the text and/or graphics, which may alter content. The journal's standard Terms & Conditions and the Ethical guidelines still apply. In no event shall the Royal Society of Chemistry be held responsible for any errors or omissions in this *Accepted Manuscript* or any consequences arising from the use of any information it contains.

ROYAL SOCIETY OF CHEMISTRY

www.rsc.org/methods

Cite this: DOI: 10.1039/c0xx00000x

www.rsc.org/xxxxxx

ARTICLE TYPE

Synthesis of sunflower-like gold nanostructure and its application in the electrochemical immunoassay using nanogold-triggered hydrogen evolution reaction†

Xiaohong Fu,* Kun Xu and Xueru Feng

Received (in XXX, XXX) Xth XXXXXXXXX 20XX, Accepted Xth XXXXXXXXX 20XX
DOI: 10.1039/b000000x

A novel and unconventional electrochemical immunosensing protocol was designed for the sensitive monitoring of neuron-specific enolase (NSE, as a model analyte) by using sunflower-like gold nanostructure (AuSF)-triggered hydrogen evolution reaction (HER).

Hydrogen evolution reaction (HER) is the main reaction in water electrolysis, and has been one of the most extensively studied electrochemical processes.[1-3] Typically, the efficiency of electrolytic hydrogen production could be improved by using some novel (nano)materials with good electrocatalytic activity.[4-6] Unfavorably, most HER reactions were applied in the energy fields for the production of hydrogen nowadays. To the best of our knowledge, there are little reports focusing on development of HER-based analytical methods, especially for immunoassay development.[7-9] Despite the high sensitivity of traditional enzyme immunoassays, they have some limitations, *e.g.*, most are susceptible to interference and assay conditions during the signal-generation stage such as pH, temperature and instability cause by structural unfolding.[10] Hence, an alternative immunosensing strategy that is based on a HER principle and does not need an enzyme labeling/or reaction process would be advantageous.

Generally, an advanced catalyst for HER should reduce the over-potential and consequently increase the efficiency of this important electronic process.[11] Gold colloids display inherent merits, *e.g.*, easy preparation, good biocompatibility and electrocatalytic activity. Merkoci's group studied the effects of gold nanoparticles-induced HER on electrocatalytic properties in electrochemical immunoassays.[7-9] However, we found that the nanostructures with different shapes usually exhibited various electrocatalytic behaviors. Mohanty et al., reported that flower-like platinum nanoparticles have superior catalytic activity for Suzuki-Miyaura and the Heck coupling reaction over spherical counterparts.[12] Qian et al. demonstrated that gold-platinum bimetallic nanoflowers could exhibit good electrocatalytic activities toward oxygen reduction.[13] To this end, our motivation in this work is to synthesize sunflower-like gold nanostructures for the advanced development of HER-based electrochemical immunoassay without the participation of natural enzymes while preserving the essential benefits in sensitivity and robustness.

Neuron-specific enolase (NSE) is detected as a substance in patients with certain tumors, namely neuroblastoma, small cell lung cancer, medullary thyroid cancer, carcinoid tumors, pancreatic endocrine tumors and melanoma. Herein we used NSE as a model for fabrication of HER-based immunoassay. To construct such an immunoassay mode, sunflower-like gold nanostructures (AuSFs) were first synthesized in aqueous solution with poly(vinyl pyrrolidone) (PVP)-sodium dodecyl sulfate (SDS) aggregations.[14] Briefly, 50-mg PVP and 35-mg SDS were added into 10-mL distilled water in a beaker under vigorous stirring in sequence. Afterwards, the mixture was heated up to 40 ºC and continuously stirred for 60 min. 50 μL of 10 mM $HAuCl_4$ aqueous solution was rapidly injected to the mixture. Following that, 1.0 mL of 50 mM NaOH solution was slowly dropped to the resulting suspension under the same conditions (*Note*: The color of the mixture changed from pale white to dark blue during this process). After that, AuSFs were collected by centrifugation (15 min at 10,000 g). Finally, the as-synthesized AuSFs were utilized for the labeling of polyclonal rabbit anti-human NSE antibody (AuSF-pAb) by the dative binding between gold nanostructures and free –SH group of the antibody (please see the similar procedure in our previous work[15]).

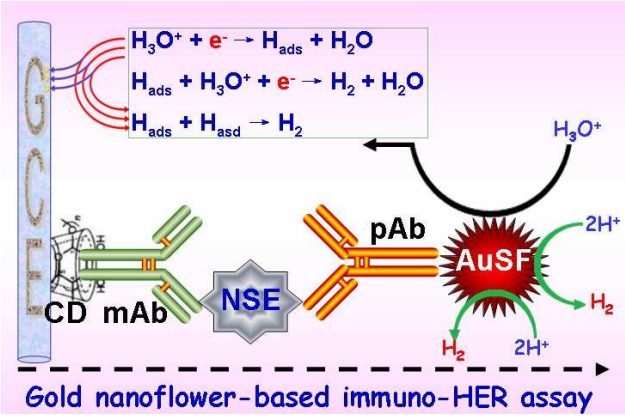

Scheme 1 Schematic illustration of the electrochemical immuno-HER assay toward neuron-specific enolase (NSE) on the monoclonal anti-NSE antibody (mAb)-modified glassy carbon electrode (GCE) using polyclonal anti-NSE antibody (pAb)-conjugated sunflower-like gold nanostructure (AuSF) as the detection antibody accompanying nanogold-triggered hydrogen evlution reaction (HER): reaction mechanism of HER (top) and immunoassay mode (bottom).

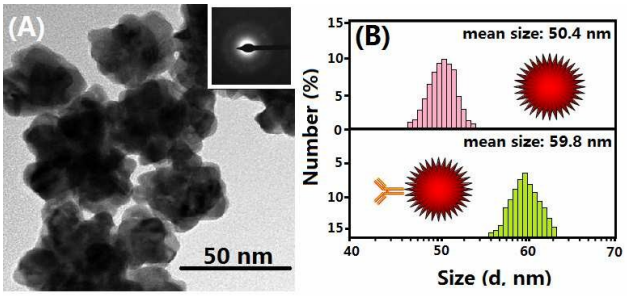

Fig. 1. (A) TEM image of the synthesized flower-like nanogold particles (inset: SAED pattern), and (B) DLS analysis of (top) AuSF and (bottom) AuSF-pAb.

To investigate the possible application of the as-prepared AuSF-pAb in the immuno-HER assay, a sandwich-type assay was designed for the detection of NSE on monoclonal mouse anti-human NSE antibody and β-cyclodextrin-modified glassy carbon electrode (2 mm in diameter, electrode area: 3.14 mm^2) (mAb-CD-GCE) (Scheme 1), using AuSF-pAb conjugates as the detection antibodies. First, a cleaned GCE was cycled in a 0.1 M H_2SO_4 solution for 5 times in the potential range from 0 to 2 V. During this process, the anodization of the GCE surface resulted in a multilayer oxide film having –OH groups or –COOH groups.[16,17] Following that, 5 μL of CD aqueous solution (50 mg/mL) was cast onto the surface of the pretreated GCE and dried for about 2 h at room temperature to form a CD-modified GCE. After being washed with distilled water, 10 μL of mAb antibodies (1.0 mg/mL) was thrown on the modified electrode, and incubated for 4 h at room temperature. During this process, mAb antibodies were immobilized on the CD-modified GCE owing to β-cyclodextrin capture.[18,19] Finally, the mAb-CD-GCE was used for the detection of NSE. In the presence of target NSE, the immobilized mAb antibody sandwiched the target analyte with the labeled pAb antibody on the AuSF. The carried gold nanostructures accompanying pAb antibody could catalyze the hydrogen evolution reaction of H^+ ions to H_2 in an acidic medium (2 M HCl used in this case), thereby resulting in the generation of electrochemical signal at the applied potential thanks to the catalytic effect of the labeled AuSFs (Please see the detailed experimental procedure in the ESI†). The signal depended on the concentration of target NSE in the sample. By monitoring the electronic signal, we could indirectly evaluate the NSE level in the detection solution.

To successfully develop the electrochemical immuno-HER assay, one important precondition was whether AuSFs could be readily synthesized by the *in situ* reduction method. To monitor this issue, we used transmission electron microscope (TEM) to characterize the as-synthesized nanostructures. As shown in Fig. 1A, the as-prepared nanostructures exhibited the sunflower-like structures with the mean size of 50 nm, which was in accordance with the result obtained from dynamic light scatter (DLS) (Fig. 1B). The inset in Fig. 1A displays the selected-area electron diffraction (SAED) pattern of the as-synthesized AuSFs, and the bright diffraction rings could be indexed as the lattice planes of a gold-face-entered-cube (fcc) lattice structure. Moreover, the size of AuSFs after conjugation with pAb antibody was obviously more than that of AuSFs alone (Fig. 1B, bottom *vs*. top). Furthermore, we also observed that the AuSFs could be homogeneously dispersed in the distilled water, thus providing the facilitation for the development of the immuno-HER.

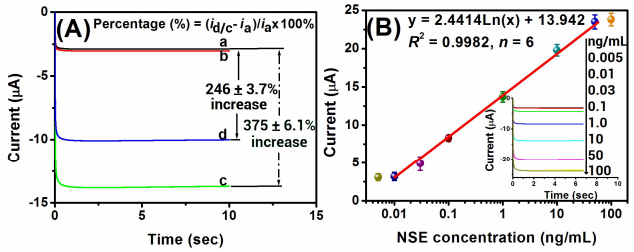

Fig. 2. (A) Chronoamperograms of (a) the newly prepared mAb-CD-GCE, (b) sensor '*a*' + AuSF-pAb, (c) sensor '*a*' + 1.0 ng/mL NSE + AuSF-pAb and (d) sensor '*a*' + 1.0 ng/mL NSE + AuNP-pAb in 2 M HCl; (B) the calibration plots of the immuno-HER assay toward NSE standards with AuSF-pAb (inset: the corresponding chronoamperometric curves).

Logically, two concerns arise as to whether (i) the prepared AuSF-pAb could be used for NSE detection on the mAb-CD-GCE, and (ii) AuSF-pAb could be non-specifically adsorbed on the mAb-CD-GCE. To clarify these points, the same-batch prepared immunosensors were employed for the detection of 0 and 1.0 ng/mL NSE using chronoamperometric assay method under the same conditions in 2.0 M HCl, respectively (Fig. 2A). Curve '*a*' gives the chronoamperometric response of newly prepared mAb-CD-GCE. In contrast, the steady-state current (curve '*b*') was almost the same as curve '*a*' when the mAb-CD-GCE was incubated with zero analyte and AuSF-pAb in turn, indicating the ignorable non-specific reaction. However, the steady-state current largely increased in the presence of 1.0 ng/mL NSE (curve '*c*'). The results revealed that the change in the current stemmed from the specific antigen-antibody reaction, *i.e.*, our strategy could be used for NSE detection.

To further monitor the amplified efficiency of AuSF-based immuno-HER assay, we prepared a kind of 50-nm spherical nanogold particles, which was used for the labeling of pAb (AuNP-pAb) (*Note*: AuNPs were synthesized referring to the literature[20]). Following that, AuSF-pAb and AuNP-pAb were used for detection of 1.0 ng/mL NSE (as an example) on the mAb-CD-GCE by using the same assay protocol, respectively. The evaluation was based on the change in the current relative to background signal. As shown in Fig. 2A, use of AuSF-pAb could cause a 375 ± 6.1% signal increase of the immuno-HER assay (curve '*c*' *vs*. curve '*a*'), whilst the signal of using AuNP-pAb only increased 246 ± 3.7% (curve '*d*' *vs*. curve '*a*'). The reason might be the fact that AuSF exhibited a dendritic structure and was more liable to form sequential field besides the adsorbed concentration/directional effect and quantum size effect. AuNF-based enzyme-free electrochemical immunoassay procedure can be simply summarized as follows:

Immunoreaction:

$$\text{NSE} + \text{mAb-CN-GCE} \rightarrow \text{NSE/mAb-CD-GCE} \quad (1)$$

$$\text{NSE/mAb-CD-GCE} + \text{pAb-AuSF} \rightarrow \text{AuSF-pAb/NSE/mAb-CD-GCE} \quad (2)$$

According to the electrochemical (EC) mechanism, the electronic signal, *i.e.*, the overall HER mechanism in acidic media occurred *via* three possible steps.[11] The first step is a primary discharge

step [$H_3O^+ + e^- \rightarrow H_{ads} + H_2O$ (Volmer reaction)], while the second step is an electrochemical desorption step [$H_{ads} + H_3O^+ + e^- \rightarrow H_2 + H_2O$ (Heyrovsky reaction)], and the third step is as recombination reaction [$H_{ads} + H_{ads} \rightarrow H_2$ (Tafel reaction]. The electrochemical desorption is a rate-determining step with the Volmer-Heyrovsky mechanism for HER.

To achieve a high sensitivity and good analytical properties, some experimental conditions including the incubation time for the antigen-antibody reaction and the applied potential for the HER reaction should be studied. Usually, the antigen-antibody reaction is adequately carried out at human normal body temperature (37 °C). However, considering the possible application of the immuno-HER assay in the future, we selected room temperature (25 ± 1.0 °C) for the antigen-antibody interaction throughout the experiment. At this condition, we monitored the effect of the incubation time on the catalytic current of the immuno-HER assay from 10 min to 50 min (*Note*: To avoid confusion, the incubation times of the immunosensor with target NSE were paralleled with those of the immunosensor-NSE with AuSF-pAb) (1.0 ng/mL NSE used as an example). As seen from Fig. S1 in the ESI†, the currents increased with the increment of incubation time, and tended to level off after 30 min. Hence, an incubation time of 30 min was selected for sensitive detection of NSE in this work.

Fig. S2 (in the ESI†) displays the effect of applied potential on the catalytic currents of the immuno-HER assay for the detection of 1.0 ng/mL NSE. The steady-state currents increased gradually with the applied potential shifted negatively from +0 to -1.0 V, which might be attributed to the increasing driving force for the fast reduction of nanocatalysts at a low potential. When the applied potential was lower than -1.0 V, the reduction current decreased gradually. So, -1.0 V was selected as the working potential for the hydrogen evolution reaction.

Using AuSF-pAb as the nanotags, the sensitivity and dynamic range of the electrochemical immuno-HER assay were evaluated on mAb-CD-GCE toward NSE standards in 2 M HCl solution with a sandwich-type immunoassay format. As seen from Fig. 2B, the steady-state currents increased with the increasing NSE levels. A linear dependence between the catalytic currents and the logarithm of NSE was obtained within the range from 0.01 to 50 ng/mL. The linear regression equation was I (μA) = 2.4414 × lg $C_{[NSE]}$ + 13.942 (ng/mL) (R^2 = 0.9982, n = 18). A detection limit of 5.0 pg/mL NSE was estimated to be 3× the standard deviation of zero-dose response, which coincided with the lower bound of the pseudolinear part of the calibration curve. Higher or lower NSE concentrations would deviate from the linear relations presumably due to that the unbalance of the ratio of antigen to antibody may result in a decreased formation of "lattice-like" immunocomplex, which was also termed as the "prozone" phenomenon in immunology.[21,22] Although the system has not yet been optimized for maximum efficiency, the LOD of using AuSF-pAb was partial lower than that of commercially available human NSE ELISA kits from CusaBio Biotech. Inc. (0.39 ng mL^{-1}), MyBioSource, Inc. (0.39 ng mL^{-1}, Cat# MBS704796, USA), Wuhan EIAab Sci. Co., Ltd (0.156 ng mL^{-1}, Cat# E0537h, China), Diagnostic Automation, Inc. (15 ng mL^{-1}, Cat# 6334Z, USA), USCN Life Sci. Inc. (0.0072 ng mL^{-1}, Cat# E90537Hu, USA), and Alpha Diagnostic Intl. (1.0 ng mL^{-1}, Cat# 0050, USA). Significantly, the system was capable of continuously carrying our all steps in about 60 min for one sample, including incubation, washing, HER reaction and measurement, which is lower than that of commercialized ELSIA kit (~3 h).

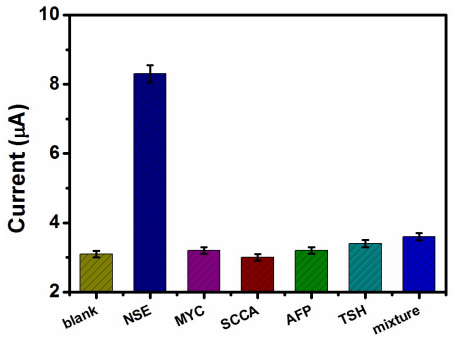

Fig. 3. The specificity of AuSF-based immuno-HER assay against 0.1 ng/mL target NSE, 100 ng/mL MYC, 100 ng/mL SCCA, 100 ng/mL AFP, 100 ng/mL TSH (*Note*: Sample mixture contained the above-mentioned analytes with the same concentrations).

The precision of the electrochemical immuno-HER assay was evaluated by repeated assaying three NSE levels, using identical batches of pAb-AuNF and mAb-CD-GCE. Experimental results indicated that the coefficients of variation (CVs) of the intra-assay (n = 3) toward 0.05 ng/mL, 1.0 ng/mL and 30 ng/mL NSE were 9.7%, 5.9% and 8.3%, respectively, whereas the CVs of the inter-assay with various-batch pAb-AuNF and mAb-CD-GCE were 10.3%, 8.7% and 9.2% toward the above-mentioned analytes, respectively. The low CVs indicated that the electrochemical immunoassay could be used repeatedly, and further verified the possibility of batch-to-batch preparation.

Further, we evaluated the specificity of the immuno-HER assay through challenging other proteins, *e.g.* myc-oncogene (MYC), squamous cell carcinoma antigen (SCCA), alpha-fetoprotein (AFP), and thyroid-stimulating hormone (TSH). Results indicated that all the interfering materials did not cause significant increase in the current relative to control test, regardless of target existance or not (Fig. 3). So, the selectivity of our strategy was acceptable.

Finally, our strategy was used for analysis of five NSE human serum specimens (*Note*: Five samples were initially detected *via* Electrochemiluminescent Automatic Analyzer and provided by Chengdu Secondary People's Hospital, China). The assayed results were 0.12, 32.4, 13.7, 3.54 and 23.6 ng/mL for sample 1-5 toward the immuno-HER assay, and 0.14, 31.2, 12.6, 3.83 and 21.5 ng/mL for Electrochemi-luminescent method, respectively. The RSDs between two methods were 10.9, 2.7, 5.9, 5.6 and 6.6% for sample 1-5, respectively, indicating that the immuno-HER assay could be used for analytical application in real samples.

In conclusion, we developed a new enzyme-free immuno-HER assay with sensitivity enhancement for electrochemical detection of NSE by using AuSF-catalyzed hydrogen evolution reaction. The signal was amplified by sunflower-like gold nanostructures. Highlight of this work is to utilize the catalytic characteristic of inorganic nanostructures, and avoid the participation of natural enzymes for the signal amplification compared with conventional

enzyme immunoassays. Importantly, the immuno-HER assay was relatively simple, low-cost and user-friendly without the need of sophisticated instruments, thereby representing a versatile detection protocol.

Support by the Natural Science Foundation of Sichuan Province (2014JY0117 & 2013sz0054), and the Excellent Talent Project of Chengdu Normal University (yjrc2012-1) is gratefully acknowledged.

Notes and references

Department of Chemistry and Bioscience, Chengdu Normal University, Chengdu 611130, P.R. China. Fax: +86 28 6677 2041; Tel: +86 28 6677 2040; E-mail: xiaohong.fuzq@gmail.com (X. Fu)

† Electronic supplementary information (ESI) available: Experimental procedures. See DOI: 10.1039/xxxxxxx

1. S. Kaufhold, L. Petermann, R. Staehle and S. Rau, *Coord. Chem. Rev.*, 2015, **304-305**, 73.
2. T. Xu, D. Chen and X. Hu, *Corrd. Chem. Rev*., 2015, **303**, 32.
3. H. Yang, Y. Zhang, F. Hu and Q. Wang, *Nano Lett*., 2015, **15**, 7616.
4. J. Zhang, L. Zhao, A. Liu, X. Li, H. Wu and C. Lu, *Electrochim. Acta*, 2015, **182**, 652.
5. B. Cao, G. Veith, J. Neuefeind, R. Adzic and P. Khalifah, *J. Am. Chem. Soc.*, 2013, **135**, 19186.
6. Q. Meng, J. Zhong, Q. Liu, X. Gao, H. Zhang, T. Lei, Z. Li, K. Feng, B. Chen, C. Tung and L. Wu, *J. Am. Chem. Soc.*, 2013, **135**, 19052.
7. C. Martinze, A. Garcia and A. Merkoci, *Biosens. Bioelectron*., 2015, **67**, 53.
8. de la Escosura, Z. Plichta, D. Horak and A. Merkoci, *Biosens. Bioelectron*., 2015, **67**, 162.
9. A. Hassan, A. de la Escosura and A. Merkoci, *Biosens. Bioelectron*., 2015, **67**, 511.
10. B. Zhang, D. tang, R. Goryacheva, R. Niessner and D. Knopp, *Chem. Eur. J.*, 2013, **19**, 2496.
11. X. Cao, Y. Han, C. Gao, Y. Xu, X. Huang, M. Willander and N. Wang, *Nano Energy*, 2014, **9**, 301.
12. A. Mohanty, N. Gary and R. Jin, *Angew. Chem., Int. Ed.*, 2010, **49**, 4962.
13. L. Qian, X. Yang, *J. Phys. Chem. B* 2006, **110**, 16672.
14. Y. Ren, C. Xu, M. Wu, M. Niu and Y. Fang, *Colloids Surf. A*, 2011, **380**, 222.
15. X. Fu, K. Xu, J. Ye, J. Chen and X. Feng, *Anal. Methods*, 2015, **7**, 507.
16. J. Tang, L. Hou, D. Tang, B. Zhang, J. Zhou and G. Chen, *Chem. Commun*., 2012, **48**, 8180.
17. X. Fu, R. Huang, J. Wang and X. Feng, *Anal. Methods,* 2013, **5**, 3803.
18. L. Zeng, Q. Li, D. Tang, G. Chen and M. Wei, *Electrochim. Acta* ,2012, **68**, 158.
19. K. Ikura, J. Fujimoto, K. Kubonishi, S. Natsuka, H. Hashimoto, T. Ito and K. Fujita, *Cytotechnology*, 2002, **40**, 23.
20. R. Yuan, D. Tang, Y. Chai, X. Zhong, Y. Liu and J. Dai, *Langmuir*, 2004, **20**, 7240.
21. M. Atassi, C. Van-Oss and D. Absolom, *Molecular Immunology*, Marcel Dekker, New York 1984
22. D. Tang and J. Ren, *Electroanalysis*, 2005, **17**, 2208.

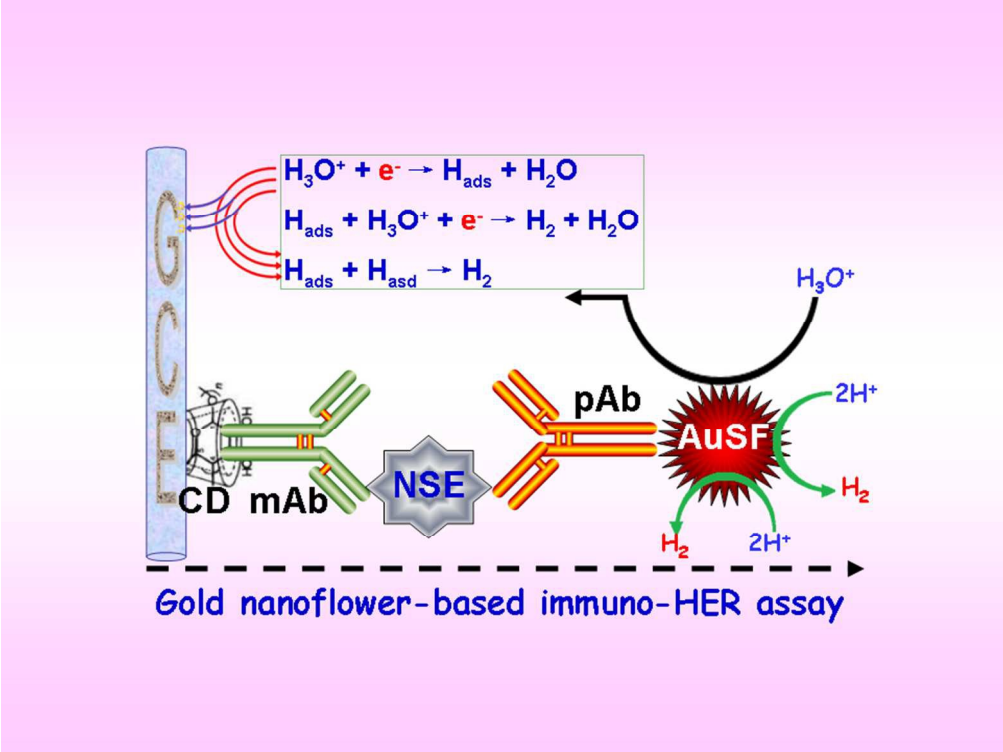

254x190mm (96 x 96 DPI)